

Article

Revealing the Critical Role of Global Electron Density Transfer in the Reaction Rate of Polar Organic Reactions within Molecular Electron Density Theory

Luis R. Domingo *  and Mar Ríos-Gutiérrez * 

Department of Organic Chemistry, University of Valencia, Dr. Moliner 50, 46100 Burjassot, Valencia, Spain

* Correspondence: luisrdomingo@gmail.com (L.R.D.); m.mar.rios@uv.es (M.R.-G.)

Abstract: The critical role of global electron density transfer (GEDT) in increasing the reaction rate of polar organic reactions has been studied within the framework of Molecular Electron Density Theory (MEDT). To this end, the series of the polar Diels–Alder (P-DA) reactions of cyclopentadiene with cyanoethylene derivatives, for which experimental kinetic data are available, have been chosen. A complete linear correlation between the computed activation Gibbs free energies and the GEDT taking place at the polar transition state structures (TSs) is found; the higher the GEDT at the TS, the lower the activation Gibbs free energy. An interacting quantum atoms energy partitioning analysis allows for establishing a complete linear correlation between the electronic stabilization of the electrophilic ethylene frameworks and the GEDT taking place at the polar TSs. This finding supports Parr’s proposal for the definition of the electrophilicity ω index. The present MEDT study establishes the critical role of the GEDT in the acceleration of polar reactions, since the electronic stabilization of the electrophilic framework with the electron density gain is greater than the destabilization of the nucleophilic one, making a net favorable electronic contribution to the decrease in the activation energy.

Keywords: global electron density transfer; molecular electron density theory; polar reactions; interacting quantum atoms; interacting quantum fragments; theoretical chemistry



Citation: Domingo, L.R.; Ríos-Gutiérrez, M. Revealing the Critical Role of Global Electron Density Transfer in the Reaction Rate of Polar Organic Reactions within Molecular Electron Density Theory. *Molecules* **2024**, *29*, 1870. <https://doi.org/10.3390/molecules29081870>

Academic Editor: Benedito José Costa Cabral

Received: 27 March 2024

Revised: 16 April 2024

Accepted: 17 April 2024

Published: 19 April 2024



Copyright: © 2024 by the authors. Licensee MDPI, Basel, Switzerland. This article is an open access article distributed under the terms and conditions of the Creative Commons Attribution (CC BY) license (<https://creativecommons.org/licenses/by/4.0/>).

1. Introduction

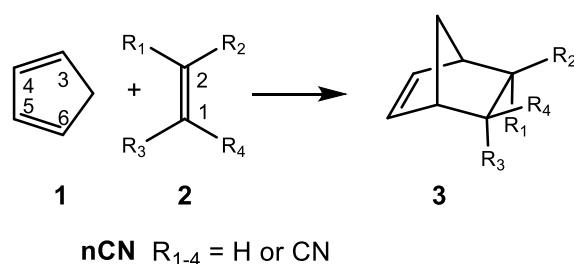
One of the most useful classifications of organic reactions is into non-polar and polar reactions. While non-polar reactions are experienced mainly by hydrocarbons, most polar reactions are characteristic of organic molecules presenting carbon-heteroatom functional groups. Unsaturated hydrocarbon compounds also experience polar reactions when they are adequately substituted by electron-withdrawing or electron-releasing groups. The polar character determines the rate of an organic reaction; while non-polar reactions have high activation energies, in general the more polar, the faster the reaction.

The idea of polar reactions in organic chemistry was introduced at the beginning of the last century. The introduction of the terms ‘nucleophile’ and ‘electrophile’ as chemists use them today is officially attributed to C. K. Ingold [1], who replaced the terms ‘anionoid’ and ‘cationoid’ proposed earlier by A. J. Lapworth in 1925 [2]. The nucleophilicity and electrophilicity concepts were further extended to reactions, and thus there are now so-known electrophilic and nucleophilic attacks, additions, substitutions, etc. [3].

From a theoretical point of view, the implementation in 1999 of the Parr’s electrophilicity ω index [4] within conceptual DFT [5,6] was a breakthrough in the theoretical understanding of polar reactions. Thus, in 2002, in an attempt to classify the Diels–Alder (DA) reactions within the polar organic reactions, the first scale of the Parr’s electrophilicity ω index of organic molecules was established, allowing to explain the substituent effects on the diene and the ethylene in the reaction rate [7]. The polar reactivity model of DA reactions was extended to [2+2], [3+2], [5+2], and so on, cycloaddition reactions. After the

study of many organic reactions, the empirical nucleophilicity N index was proposed in 2008 [8] which, together with the electrophilicity ω index, have become powerful tools to study the polar reactivity in organic chemistry [9].

In 1964, Sauer et al. [10] experimentally reported the reactivity of Cp **1** with the cyanoethylene series **2** in DA reactions (see Scheme 1). The reported experimental reaction rate constants have been used in organic chemistry textbooks to show how the electron-withdrawing substitution on ethylene increases the reaction rates of DA reactions (see Table 1) [11].



Scheme 1. DA reactions between Cp **1** and the cyanoethylene series **2**, reported in 1964 by Sauer et al. [10].

Table 1. Reaction rate constants for the P-DA reactions of Cp **1** with the cyanoethylene series **2**^{a,b}.

	Ethylene Derivative	$10^5 k [\text{M}^{-1}\text{s}^{-1}]$
4CN	tetracyanoethylene	4.3×10^7
3CN	tricyanoethylene	4.8×10^5
2CN	1,1-dicyanoethylene	4.5×10^4
2cCN	maleonitrile	91
2tCN	fumaronitrile	81
1CN	acrylonitrile	1.04

^a At 20 °C in dioxane. ^b The rate constant for the Cp **1** + ethylene **4** DA reaction has been estimated to be 10^{-5} .

The Sauer's DA reactions of the cyanoethylene series have been theoretically studied [11,12]. A very good linear correlation between the global electron density transfer [13] (GEDT) taking place at the transition state structures (TSs) [11] and the logarithm of the experimental reaction rate constants [10] was established for the first time in 2009 [14], indicating that the GEDT could be one of the key factors in the activation energy (see Figure 1).

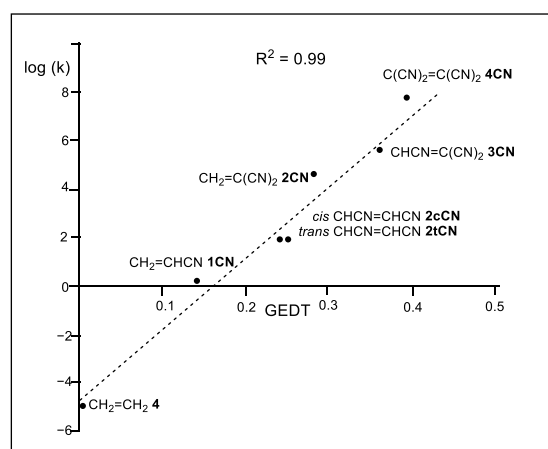


Figure 1. Plot of the logarithm of the experimental reaction rate constant k , in dioxane, vs. GEDT, in average number of electrons, e , for the DA reactions of Cp **1** with ethylene **4** and the cyanoethylene series **2**.

After many theoretical studies of experimental DA reactions, a very good linear correlation between the activation energies of DA reactions and the GEDT taking place at the TSs was recognized in 2009, thus establishing the general mechanism of polar Diels–Alder (P-DA) reactions [14], which are controlled by the nucleophilic and electrophilic interactions taking place at the TSs. In polar reactions, the increase in GEDT at the TSs causes a decrease in the activation energies, increasing the reaction rates [11,14]. This behavior has been found in many polar organic reactions such as [2+2] and [3+2] cycloaddition reactions, Lewis acid-catalyzed DA reactions, higher-order cycloaddition reactions, Michael reactions, Wittig reactions, and electrophilic aromatic substitution reactions.

In 2017, a comparative electron localization function [15] (ELF) and Quantum Theory of Atoms in Molecules [16,17] (QTAIM) topological analysis of the TSs of the DA reactions of Cp **1** with ethylene **4** and with tetracyanoethylene **4CN** [18] showed that in the polar reaction involving **4CN**, the GEDT favors the bonding changes on the reagents demanded for the formation of the new C–C single bonds [13], allowing the TS to occur earlier [18]. However, the effects of the GEDT in the reduction in the activation energies could not be established.

In 2016, Domingo proposed the Molecular Electron Density Theory [19] (MEDT) for the study of chemical organic reactivity. MEDT establishes that changes in electron density along a reaction, and not molecular orbital interactions, are responsible for chemical reactivity. Accordingly, MEDT rejects any model based on molecular orbital analyses, such as the Frontier Molecular Orbital theory [20] and Morokuma-based energy decomposition schemes [21,22], all of which were developed in the last century.

In 2005, Blanco et al. developed a parameter-free and reference-free energy decomposition scheme based on QTAIM, called interacting quantum atoms [23] (IQA). IQA divides the total energy of a system into intra- and inter-atomic contributions, each of a different nature, which are related to chemical concepts of bonding. IQA analysis has very recently been used in MEDT studies of [3+2] cycloaddition reactions [24] and P-DA reactions [25].

Due to the relevance of the GEDT taking place at the TSs of polar reactions in organic chemistry [11], an MEDT/IQA study of the P-DA reactions of Cp **1** with the Sauer's cyanoethylene series **2**, as models of polar organic reactions, is herein performed in order to definitively establish the critical role of GEDT in the acceleration in polar processes both qualitatively and quantitatively. To this end, an IQA energy partitioning analysis at the TSs and reagents is carried out. The conclusions of this study can be extrapolated to any organic polar reaction.

2. Results and Discussion

This section has been divided in the following subsections: (i) first, the DFT-based reactivity indices of the reagents are analyzed; (ii) next, kinetic, thermodynamic, and geometrical parameters associated with the P-DA reactions of Cp **1** with the cyanoethylene series **2** are discussed, along with some correlations involving electrophilicities and GEDT values; and finally, (iii) a density-based IQA energy partitioning analysis is performed in order to establish, both quantitatively and qualitatively, the role of GEDT in increasing the reaction rates with the cyano substitution on the ethylene. Except for kinetic and thermodynamic data, which are analyzed in dioxane for comparison with the experiment, all other analyses are discussed in vacuo for coherence with the IQA analysis, which does not yet support the implicit effect of solvent in atomic integrations (see the Computational Details in Supplementary Materials).

2.1. Analysis of the Reactivity Indices at the Ground State of the Reagents

The reactivity indices [5,6] for Cp **1** and the cyanoethylene series **2** computed at the ground state are gathered in Table 2. Computational details are given in Supplementary Materials. The B3LYP/6-31G(d) computational method was used because the original reactivity scales were established at that level [5,6]. Analysis of the electronic chemical potentials [26] μ of the reagents allows for establishing of the polar character of an organic

reaction, as well as the unambiguous establishment of the direction of the flux of the electron density, which enables the classification of polar reactions [27,28]. The electronic chemical potential μ of Cp **1**, -3.01 eV, is above those of the cyanoethylene series **2**, between -4.70 (**1CN**) and -7.04 (**4CN**) eV, indicating that in these polar reactions the electron density will flux from Cp **1** towards these cyanoethylenes, being classified as P-DA reactions of forward electron density flux [27,28].

Table 2. In vacuo B3LYP/6-31G(d) global electronic chemical potential μ , chemical hardness η , electrophilicity ω , and nucleophilicity N , in eV, of Cp **1** and the cyanoethylene series **2**.

	μ	η	ω	N
4CN	-7.04	4.16	5.95	0.00
3CN	-6.43	4.71	4.39	0.33
2tCN	-5.71	5.29	3.08	0.76
2cCN	-5.66	5.32	3.01	0.80
2CN	-5.64	5.65	2.82	0.65
1CN	-4.70	6.34	1.74	1.25
Cp 1	-3.01	5.49	0.83	3.37
Ethylene 4	-3.37	7.77	0.73	1.87

Cp **1** presents an electrophilicity ω index [4] of 0.83 eV and a nucleophilicity N index [8] of 3.37 eV, being classified as a moderate electrophile and a strong nucleophile. Consequently, Cp **1** will participate in P-DA reactions only as a good nucleophile. On the other hand, ethylene **4** presents an electrophilicity ω index of 0.73 eV and a nucleophilicity N index of 1.87 eV, being classified as a marginal electrophile and a marginal nucleophile. Consequently, ethylene **4** will never participate in a P-DA reaction. The non-polar Diels–Alder (N-DA) reaction of Cp **1** with ethylene **4** is classified within MEDT as a null electron density flux reaction [28].

The electrophilicity ω index of cyanoethylene series **2** ranges from 1.74 eV (**1CN**) to 5.95 eV (**4CN**), while the nucleophilicity N index ranges from 1.25 eV (**1CN**) to 0.00 eV (**4CN**). Note that the nucleophilicity N index for **4CN** is exactly 0.00 eV because this molecule was chosen as the reference for the empirical nucleophilicity N scale [6,9]. Thus, while **1CN** is located on the borderline between moderate electrophiles, the other cyanoethylenes are clearly classified as strong electrophiles; note that the tri- and tetracyanoethylenes **3CN** and **4CN**, with $\omega > 4.0$ eV, are classified as superelectrophiles, a behavior that accounts for their high reactivity in polar processes [9] (see Table 1). On the other hand, all cyanoethylenes are classified as marginal nucleophiles. Consequently, this cyanoethylene series will participate towards Cp **1** in P-DA reactions of forward electron density flux [27,28]. Both electrophilic and nucleophilic properties of this series vary with the number of cyano groups on the ethylene.

Along a polar cycloaddition reaction involving non-symmetric species such as **1CN**, **2CN** or **3CN**, the most favorable reaction path involves the two-center interaction with the most electrophilic center of these cyanoethylenes [11]. In this sense, the analysis of the electrophilic P_k^+ Parr functions [29] of the cyanoethylene series is a valuable tool to characterize the most electrophilic center of these molecules (see Figure 2 and Table 3).

Analysis of the electrophilic P_k^+ Parr functions at the C1 and C2 carbons of the cyanoethylene series **2** indicates that the two ethylene carbons gather more than 60% of the total amount of spin density in these molecules; i.e., the two carbons will accumulate more than 60% of the electron density transferred to these ethylene derivatives via the GEDT in these P-DA reactions. As expected, the symmetrically substituted ethylenes **2cCN**, **2tCN**, and **4CN** present identical electrophilic P_k^+ Parr functions at the two carbons, while the non-symmetrically substituted **1CN**, **2CN**, and **3CN** present a non-symmetrical electrophilic activation; in the three cases, the less-substituted carbon present the higher electrophilic P_k^+ Parr function (see Table 3).

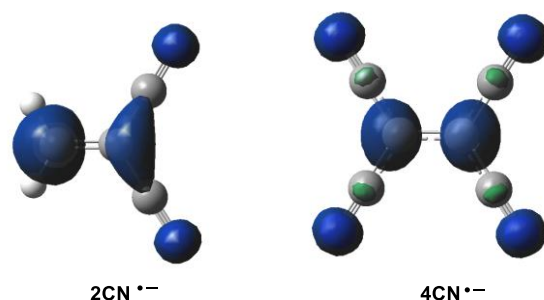


Figure 2. Three-dimensional representations of the Mulliken atomic spin densities of the radical anions of **2CN** and **4CN**.

Table 3. In vacuo B3LYP/6-31G(d) electrophilic P_k^+ Parr functions and local electrophilicity ω_k indices at the C1 and C2 carbons of the cyanoethylene series **2**.

	P_k^+		ω_k		$\Delta\omega_k$
	C1	C2	C1	C2	
1CN	0.63	0.20	1.10	0.34	0.76
2cCN	0.35	0.35	0.98	0.98	0.00
2tCN	0.33	0.33	1.01	1.01	0.00
2CN	0.74	0.10	2.28	0.30	1.98
3CN	0.46	0.22	2.03	0.94	1.09
4CN	0.32	0.32	1.91	1.91	0.00

Analysis of the local electrophilicity ω_k indices [30] at the C1 and C2 carbons of these cyanoethylenes allows for obtaining some appealing conclusions (see Table 3): (i) while the symmetrically substituted ethylenes **2cCN**, **2tCN** and **4CN** present identical electrophilic activation at the two ethylene carbons, predicting synchronous TSs, the non-symmetrically substituted **1CN**, **2CN** and **3CN** present different electrophilic activation, predicting asynchronous TSs [11]; (ii) at the non-symmetrically substituted **1CN**, **2CN** and **3CN** cyanoethylenes, the less-substituted C1 carbon presents the higher electrophilic activation, indicating that this carbon will be the preferred center to participate in the two-center interaction with the C6 carbon of the nucleophilic Cp **1** [11]; and finally, (iii) the local electrophilicity at the C1 carbon of **2CN**, $\omega_k = 2.28$ eV, is higher than that at the C1 carbon of **3CN**, $\omega_k = 2.03$ eV, despite the more electrophilic character of **3CN** than **2CN**. Note that the two C1 and C2 carbons of the symmetrically substituted **2cCN** and **2tCN** are electrophilically activated by ca. $\omega_k = 1.0$ eV, for each one.

2.2. Study of the P-DA Reactions of Cp **1** with the Cyanoethylene Series **2**

For the non-symmetrically substituted cyanoethylenes **1CN**, **2CN**, and **3CN**, two stereoisomeric reaction paths are feasible; only the *endo* approach mode was studied herein (see Scheme 1). A detailed analysis of the potential energy surfaces is found in [11]. The M06-2X/6-311G(d,p) relative Gibbs free energies of TSs and CAs in dioxane are given in Table 4, while complete thermodynamic data are given in Table S3 in Supplementary Materials.

The activation Gibbs free energies range from 25.9 (**TS-1CN**) to 12.7 (**TS-4CN**) kcal mol⁻¹. Note that the N-DA reaction of Cp **1** with ethylene **4** displays a very high activation Gibbs free energy of 29.8 kcal mol⁻¹ (see Table 4). These DA reactions are exergonic in the narrow range between -12.7 (**CA-1CN**) and -14.9 (**CA-4CN**) kcal mol⁻¹.

A representation of the activation Gibbs free energies versus the number of cyano groups on the ethylene shows a very good linear correlation with a coefficient of determination $R^2 = 0.94$ (see Figure S4 in Supplementary Materials). This graph shows that the presence of the cyano group on the ethylene is additive and has a marked effect on the kinetics of the reactions, in clear agreement with the experimental outcomes observed by Sauer et al. (see Table 1).

Table 4. M06-2X/6-311G(d,p) relative Gibbs free energies, ΔG in kcal mol⁻¹, computed at 293.15 K and 1 atm in dioxane, of TSs and CAs involved in the DA reactions of Cp **1** with ethylene **4** and the cyanoethylene series **2**. The computed relative reaction rate constant k_r , with respect to the reaction with ethylene **4**, is also included.

Reagent	TS	ΔG	k_r	Product	ΔG
Ethylene 4	TS-Et	29.8	1.00×10	CA-Et	-12.8
1CN	TS-1CN	25.9	8.09×10^2	CA-1CN	-12.7
2cCN	TS-2cCN	22.3	3.91×10^5	CA-2cCN	-13.8
2tCN	TS-2tCN	22.0	6.54×10^5	CA-2tCN	-14.5
2CN	TS-2CN	18.2	4.45×10^8	CA-2CN	-13.0
3CN	TS-3CN	15.9	2.31×10^{10}	CA-3CN	-14.9
4CN	TS-4CN	12.7	5.62×10^{12}	CA-4CN	-14.9

Using the Eyring–Polanyi equation [31], the relative reaction rate constants k_r of the P-DA reactions between Cp **1** and the cyanoethylene series **2**, with respect to that with ethylene **4**, were computed (see Table 4). The relative reaction rate constants k_r range from 8.09×10^2 (**1CN**) to 5.62×10^{12} (**4CN**). Thus, the P-DA reaction involving the superelectrophilic tetracyanoethylene **4CN** is 10^{12} faster than the N-DA reaction of Cp **1** with ethylene **4**. A representation of the logarithm of the experimental relative reaction rate constants $\log(k_{r,exp})$, with respect to the N-DA reactions of Cp **1** with ethylene **4**, versus the logarithm of the computed relative reaction rate constants $\log(k_{r,comp})$ shows a complete linear correlation with an $R^2 = 1.00$ (see Figure S5 in Supplementary Materials).

The main geometrical parameters at the in vacuo TSs, i.e., the distances between the two pairs of C1–C6 and C2–C3 interacting centers, together with the geometrical asynchronicity, Δl , and the average of the two C–C distances, l_m , are given in Table 5. Geometrical data in dioxane are gathered in Table S4 in Supplementary Materials; they show no significant changes compared to the in vacuo parameters. The geometries of two representative TSs are given in Figure 3, while the geometries of all TSs are given in Figure S6 in Supplementary Materials. Some appealing conclusions can be obtained from the geometrical data given in Table 5: (i) from a geometrical point of view, the TSs can be classified as synchronous and asynchronous TSs, depending on the evolution of the new C–C single bond formation; (ii) while the synchronous TSs, $\Delta l = 0.0$ Å, come from the symmetrically substituted ethylenes, asynchronous TSs, $\Delta l > 0.2$ Å, come from the non-symmetrically substituted ethylenes; (iii) interestingly, the average of the two C1–C6 and C2–C3 distances at all TS, including TS-Et, is 2.24 Å (see l_m in Table 5). This behavior indicates that all TSs have a comparable advanced/early character. Considering that the C–C single bond formation takes place in the short range of 2.0–1.9 Å [13], these geometrical parameters indicate that formation of the first C–C single bond has not yet started in any of the TSs (see later). This behavior is consistent with Woodward’s 1942 proposal that electron transfer occurs before the formation of the new C–C single bonds [32].

Table 5. Distances between the C1–C6 and C2–C3 interacting carbons at the M06-2X/6-311G(d,p) in vacuo optimized TSs, geometrical asynchronicity Δl , and average of the two C–C interacting distances l_m , in angstroms, Å, and GEDT values in average number of electrons, e .

	C1–C6	C2–C3	Δl	l_m	GEDT
Et	2.223	2.223	0.00	2.22	0.03
1CN	2.118	2.342	0.22	2.23	-0.14
2cCN	2.220	2.220	0.00	2.22	-0.23
2tCN	2.219	2.233	0.01	2.23	-0.23
2CN	2.025	2.535	0.51	2.28	-0.27
3CN	2.092	2.417	0.32	2.25	-0.34
4CN	2.225	2.225	0.00	2.22	-0.42

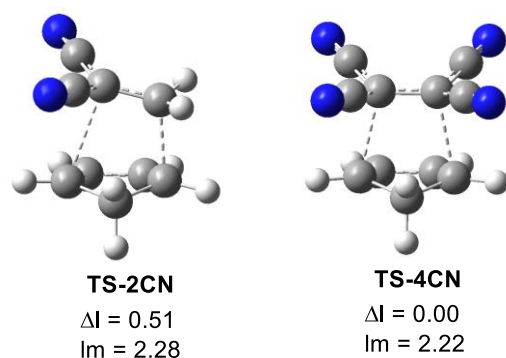


Figure 3. M06-2X/6-311G(d,p) in vacuo optimized geometries of the highly asynchronous **TS-2CN** and the synchronous **TS-4CN**. The geometrical asynchronicity Δl and the average distances, given in angstroms, \AA , are also included.

As Figure 4 shows, a complete linear correlation between the geometrical asynchronicity, Δl , of the TSs and the difference of the local electrophilicity ω_k indices of the C1 and C2 carbons of the cyanoethylenes, $\Delta\omega_k$, is established for the first time, with $R^2 = 1.00$. Thus, the symmetrically substituted cyanoethylenes **2cCN**, **2tCN** and **4CN** with $\Delta\omega_k = 0.00$ eV yield synchronous TSs, while non-symmetrically substituted cyanoethylenes **1CN**, **2CN** and **3CN** with $\Delta\omega_k > 0.76$ eV yield asynchronous TSs. This excellent relationship indicates that the different electrophilic activation of the two C1 and C2 carbons of the electrophilic ethylenes caused by the electron-withdrawing substitution controls the asynchronicity of the C–C single bond formation in these P-DA reactions.

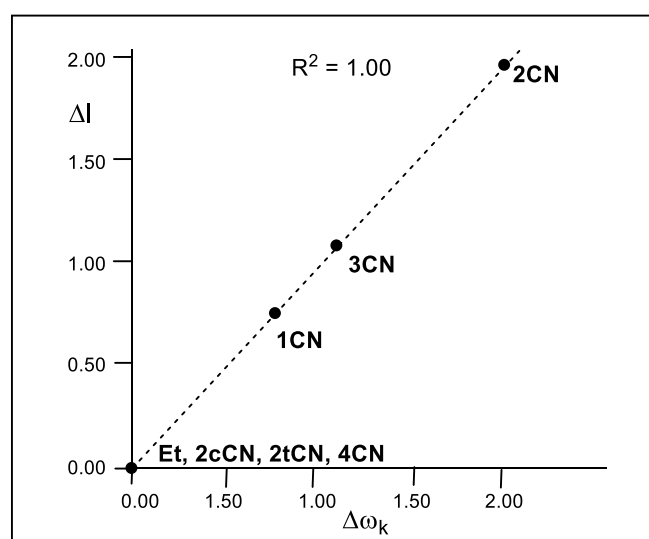


Figure 4. Plot of the in vacuo geometrical asynchronicity of the TSs, Δl in angstroms \AA , with respect to the difference of the local electrophilicity ω_k indices of the C1 and C2 carbons of the cyanoethylene series 2, $\Delta\omega_k$ in eV.

Analysis of GEDT at the TSs permits to quantify the polar character of these DA reactions [14]. The GEDT values computed at the seven TSs in vacuo are given in Table 5. GEDT values in dioxane are displayed in Table S4 in Supplementary Materials and show no significant changes compared to the in vacuo values. As expected, the GEDT value at **TS-Et** is negligible, 0.03 e, as a consequence of the marginal electrophilic character of ethylene **4** (see Table 2). Consequently, the corresponding DA reaction has a non-polar character, being classified as null electron density flux [28]. The presence of a cyano group in **1CN** notably increases the GEDT at **TS-1CN** to 0.14 e. The addition of cyano groups at the ethylene moiety markedly increases the GEDT at the corresponding TSs, reaching a

maximum value at **TS-4CN** with a GEDT = 0.42 e. These P-DA reactions are classified as FEDF [27,28], in agreement with the previous reactivity indices prediction (see Section 2.1). The presence of at least two cyano groups makes the corresponding DA reaction very polar (see Table 5). It is worth mentioning that GEDT values obtained from an NPA analysis do not significantly vary with the charge partitioning method because of its formal definition (see Computational Details in Supplementary Materials). For instance, in vacuo GEDT values computed with Bader charges show no significant variation (see in Table S4 and the linear regression in Figure S7 in Supplementary Materials).

A representation of the activation Gibbs free energies of these P-DA reactions versus the computed GEDT values at the corresponding TSs also shows a very good linear correlation with an $R^2 = 0.98$ (see Figure 5). This linear correlation, that has been found in numerous organic reactions, shows the significant role of the polar character of the reactions, measured by the computed GEDT values, in reaction rates.

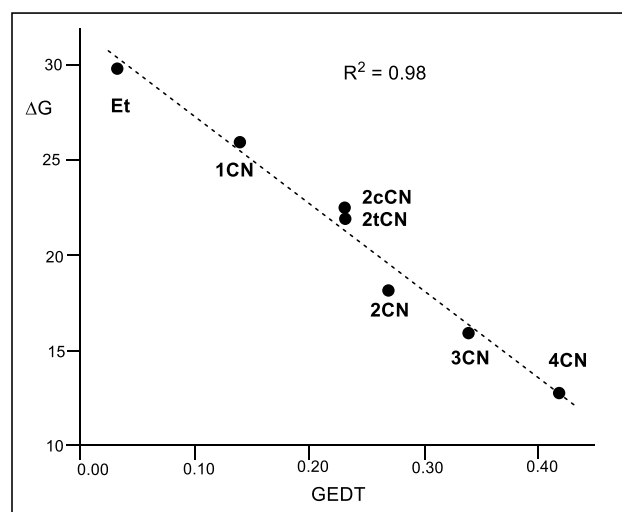


Figure 5. Plot of the M06-2X/6-311G(d,p) activation Gibbs free energies, ΔG in kcal mol^{-1} , vs. the GEDT, in average number of electrons e, $R^2 = 0.98$, for the DA reactions of Cp 1 with ethylene 4, and with the cyanoethylene series 2.

It is worth noting that although geminal **2CN** is less electrophilic than vicinal **2cCN** and **2tCN**, the reaction of **2CN** is more polar and has a higher reaction rate (see Figure 5). This finding points out, once again, the relevant role of GEDT in reaction rates, and indicates that asynchronous processes are generally preferred over synchronous ones due to a more favorable two-center interaction (see later).

Finally, ELF and QTAIM topological analyses of the electronic structures of the reagents and TSs were performed. The corresponding analyses are given in Supplementary Materials. ELF analysis of the reagents indicates that the cyano substitution on the ethylene does not cause any remarkable changes in the C–C double bond region at the ground state of these substituted ethylenes. On the other hand, ELF analysis of the TSs indicates that while the low polar **TS-1CN** and **TS-2cCN** and **TS-2tCN** show a great similitude to the non-polar **TS-Et**, the highly polar **TS-2CN**, **TS-3CN** and **TS-4CN** show the presence of the *pseudoradical* centers demanded for the subsequent C–C single bond formation [13]. Both ELF and QTAIM analyses of the electron density at the TSs indicate that formation of the C–C single bonds has not started yet in any of them, thus rejecting the concept of concerted TSs.

2.3. IQA Analysis of the TSs of the P-DA Reactions of the Cyanoethylene Series 2

In order to determine the role of the GEDT caused by the cyano substitution on the ethylene in the experimental acceleration observed by Sauer et al. (see Table 1), a topological IQA [23] energy partitioning was carried out at the seven TSs in vacuo. For this purpose,

an interacting quantum fragments approach [33] was adopted, considering relative IQA energies at both interacting frameworks as defined in Supplementary Materials. The relative total, intra- and inter-atomic IQA energies of each TS fragment are given in Table 6, while the total values are given in Table S5 in Supplementary Materials.

Table 6. M06-2X/6-311G(d,p) in vacuo relative total $E_{\text{tot}}(X)$, intra- $E_{\text{intra}}(X)$ and inter-atomic $V_{\text{inter}}(X)$ IQA energies, in kcal mol⁻¹, of the cyclopentadiene and ethylene frameworks at the TSs with respect to the separated reagents. The sum of the relative total IQA energies of the two interacting moieties, $E_{\text{tot}}(\text{Cp+Et})$, yields the activation energy. Standard deviations are given with respect to the N-DA reaction of Cp **1** with ethylene **4**, in kcal mol⁻¹.

		$E_{\text{intra}}(X)$	$V_{\text{inter}}(X)$	$E_{\text{tot}}(X)$	$E_{\text{tot}}(\text{Cp+Et})$
TS-Et	Cp	34.6	-26.8	7.8	15.6
	Et	33.1	-25.3	7.8	
TS-1CN	Cp	37.8	-19.9	17.9	11.0
	1CN	34.4	-41.3	-6.9	
TS-2cCN	Cp	42.3	-13.6	28.7	8.1
	2cCN	49.4	-70.0	-20.6	
TS-2tCN	Cp	41.8	-13.2	28.6	6.9
	2tCN	46.5	-68.2	-21.7	
TS-2CN	Cp	41.2	-10.0	31.2	4.0
	2CN	29.3	-56.5	-27.2	
TS-3CN	Cp	46.1	-4.4	41.7	1.9
	3CN	54.8	-94.6	-39.8	
TS-4CN	Cp	51.9	1.3	53.2	-1.5
	4CN	72.6	-127.3	-54.7	
Standard deviation	Cp	10.0	18.2	28.1	
	nCN	20.4	58.1	39.3	

Table 6 shows that the stabilization of the ethylene framework with the number of cyano groups, $\Delta E_{\text{tot}}(n\text{CN}) < 0$, is stronger than the Cp destabilization, $\Delta E_{\text{tot}}(\text{Cp}) > 0$, justifying the decrease in the activation energies along this cyanoethylene series. In addition, while the increase in the cyano substitution in the ethylene generally increases $E_{\text{intra}}(X)$ in the two interacting frameworks and $V_{\text{inter}}(\text{Cp})$, a huge decrease in the inter-atomic $V_{\text{inter}}(n\text{CN})$ energies, by between -16.0 (1CN) and -102.0 (4CN) kcal mol⁻¹, is observed (see the differences between $V_{\text{inter}}(n\text{CN})$ and $V_{\text{inter}}(\text{Et})$).

Figure 6 shows a graphical representation of the interacting quantum fragment $E_{\text{tot}}(X)$ energy of the Cp and Et frameworks at the seven TSs and the $E_{\text{tot}}(\text{Cp+Et})$, which corresponds to the activation energies of these DA reactions. As can be observed, both $E_{\text{tot}}(X)$ are positive and unfavorable in the N-DA reaction with ethylene **4**. However, along the cyanoethylene series **2**, the interacting quantum fragment energies associated with the Cp framework increase while those of the ethylene derivatives become more negative, i.e., more stabilizing. This stabilization reaches such an extent that, in TS-4CN, the stabilization of the ethylene framework overcomes the destabilization of the Cp one, and the corresponding relative energy of TS-4CN becomes negative. These behaviors are a consequence of the GEDT that takes place at the TSs (see Figure 6), that while it destabilizes the nucleophile Cp for making it lose electron density, it stabilizes the electrophile nCN as it gains electron density.

The activation Gibbs free energies range from 25.9 (TS-1CN) to 12.7 (TS-4CN) kcal mol⁻¹. Note that the N-DA reaction of Cp **1** with ethylene **4** displays a very high activation Gibbs free energy of 29.8 kcal mol⁻¹ (see Table 4). These DA reactions are exergonic in the narrow range between -12.7 (CA-1CN) and -14.9 (CA-4CN) kcal mol⁻¹.

A representation of the activation Gibbs free energies versus the number of cyano groups on the ethylene shows a very good linear correlation with a coefficient of determination $R^2 = 0.94$ (see Figure S4 in Supplementary Materials). This graph shows that the presence of the cyano group on the ethylene is additive and has a marked effect on the

kinetics of the reactions, in clear agreement with the experimental outcomes observed by Sauer et al. (see Table 1).

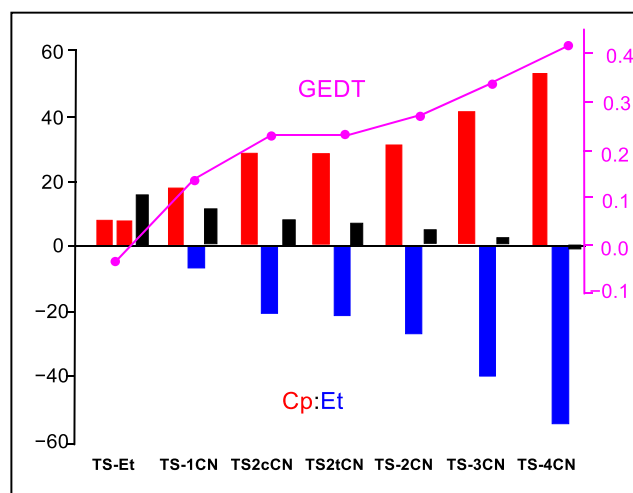


Figure 6. Graphical representation of the sets of $E_{\text{tot}}(\text{Cp})$, $E_{\text{tot}}(\text{Et})$, and $E_{\text{tot}}(\text{Cp+Et})$ energies in that order for the TSs associated with the DA reactions of Cp 1 with ethylene 4 and the cyanoethylenes series 2. $E_{\text{tot}}(\text{Cp+Et})$ corresponds to the activation energies of the reactions. The GEDT values at the TSs are given in pink. $E_{\text{tot}}(\text{X})$ energies are given in kcal mol⁻¹, and the GEDT in average number of electrons, e.

Consequently, the strong stabilization of the cyanoethylene framework at the TSs with the cyano substitution, by between 14.7 (1CN) and 62.5 (4CN) kcal mol⁻¹ with respect to the N-DA reaction of Cp 1 with ethylene 4, accounts for the decrease in the activation energies associated with the P-DA reactions between Cp 1 and the cyanoethylene series 2.

A representation of the logarithm of the experimental reaction rate constant k versus the stabilization of the ethylene frameworks at the TSs shows an excellent linear correlation with an $R^2 = 0.95$ (see Figure S8 in Supplementary Materials). This figure shows the close relationship between the experimentally observed acceleration in this series of P-DA reactions and the decrease in activation energy resulting from the electronic stabilization of the ethylene framework. Furthermore, a representation of $E_{\text{tot}}(\text{Et})$ versus the GEDT computed at the TSs shows an excellent linear correlation with an $R^2 = 0.99$ (see Figure 7).

These linear correlations allow establishing, for the first time, that the electronic stabilization of the ethylene framework, resulting from the GEDT process taking place in polar reactions, is responsible for the increase in the reaction rate observed in these polar reactions [14]. Note that the N-DA reaction of ethylene 4, which presents a GEDT = 0.03 e, fits in the top left corner in the linear regression in Figure 7.

As the energy factor that changes the most with the cyano substitution is $V_{\text{inter}}(\text{Et})$, in order to gain a more detailed insight into the stabilization of the ethylene derivatives, the inter-atomic interactions between the Cp and ethylene frameworks, $V_{\text{inter}}(\text{Cp,Et})$, were considered separately from the interactions that take place within each of them, $V'_{\text{inter}}(\text{X})$. The corresponding energies, together with the standard deviations with respect to the N-DA reaction of ethylene 4 as the reference, are given in Table 7.

The standard deviation values indicate that the most drastic changes with the cyano substitution take place in decreasing the inter-atomic interactions occurring inside the ethylene fragment (see the standard deviation of $V'_{\text{inter}}(\text{Et})$ in Table 7). This effect overcomes the changes in the inter-atomic interactions between the fragments, $V_{\text{inter}}(\text{Cp,Et})$, which also become more stabilizing as the polar character of the reaction increases.

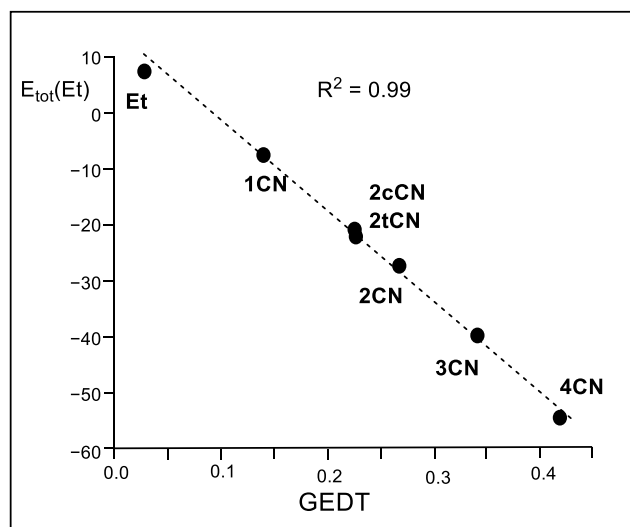


Figure 7. Plot of the in vacuo M06-2X/6-311G(d,p) relative total IQA atomic energies of the ethylene framework, $E_{\text{tot}}(\text{Et})$ in kcal mol^{-1} , vs. the GEDT, in average number of electrons e , for the DA reactions of Cp **1** with ethylene **4** and the cyanoethylene series **2**.

Table 7. M06-2X/6-311G(d,p) in vacuo total inter-atomic interactions between the two Cp and Et fragments, $V_{\text{inter}}(\text{Cp},\text{Et})$, and relative total inter-atomic energies within the two Cp and Et frameworks, $V'_{\text{inter}}(\text{X})$, in kcal mol^{-1} . Relative energies are given with respect to the separated reagents. Standard deviations are given with respect to the N-DA of Cp **1** with ethylene **4**, in kcal mol^{-1} .

	$V_{\text{inter}}(\text{Cp},\text{Et})$	$V'_{\text{inter}}(\text{Cp})$	$V'_{\text{inter}}(\text{Et})$
TS-Et	-153.7	50.0	51.5
TS-1CN	-160.4	60.4	38.9
TS-2cCN	-167.7	70.3	13.7
TS-2tCN	-168.7	71.1	16.2
TS-2CN	-165.5	72.8	26.3
TS-3CN	-174.1	82.6	-7.6
TS-4CN	-187.3	94.8	-33.6
Deviation	18.9	27.5	48.7

These findings confirm that the stabilization of the electrophilic reagent in P-DA reactions is the most relevant consequence of the GEDT, thus being responsible for the increase in reaction rates with the increase in the polar character [13].

Finally, in 1999, Parr proposed the electrophilicity ω index as a measure of the electronic stabilization of a species when it acquires a certain amount of electron density from the environment [4]. Thus, when the sum of the relative intra-atomic $E_{\text{intra}}(\text{Et})$ and inter-atomic $V'_{\text{inter}}(\text{Et})$ IQA energies, i.e., $E'_{\text{tot}}(\text{Et})$, are represented versus the corresponding Parr's electrophilicity ω indices (see Table 2), a very good linear correlation is obtained; $R^2 = 0.97$ (see Figure 8). The $E'_{\text{tot}}(\text{Et})$ in the N-DA reaction between Cp **1** and ethylene **4** is very unfavorable, $84.6 \text{ kcal mol}^{-1}$. The inclusion of the cyano groups stabilizes the ethylene framework at the TSs by between 11.3 (**1CN**) and 45.7 (**4CN**) kcal mol^{-1} as a consequence of the GEDT taking place at the polar TSs (see Figure 8). Consequently, this graph supports Parr's proposal [4,34]; the higher the electrophilicity ω index, the higher the ethylene stabilization at the polar TSs. Given that the ethylene stabilization via the GEDT is the main factor responsible for the decrease in activation energies, as shown above, this linear correlation also validates Parr's electrophilicity ω index as a solid predictor of reactivity in polar cycloaddition reactions.

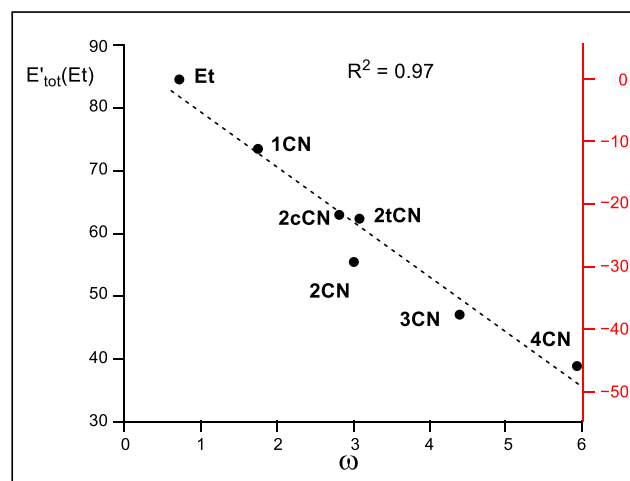


Figure 8. Plot of the M06-2X/6-311G(d,p) in vacuo relative total IQA energy at the ethylene framework, $E'_{\text{tot}}(\text{Et})$, in kcal mol^{-1} , vs. Parr's electrophilicity ω indices, in eV, of the ethylenes involved in the DA reactions of Cp **1** with ethylene **4** and the cyanoethylene series **2**. The scale of the energy differences with respect to the N-DA reaction of ethylene **4**, which measures the TS stabilization, is given in red on the right side.

3. Computational Methods

The M06-2X functional [35], together with the standard 6-311G(d,p) basis set [36], which includes d-type polarization for second-row elements and p-type polarization functions for hydrogens, was used throughout this MEDT study. In general, a careful study of DA reactions calls for the adoption of higher-level wave function models, placing more emphasis on the electron correlation effects than single-determinantal wave function methods. However, the polar character of the DA reactions studied in the present manuscript enables the single-determinant level. The TSs were characterized by the presence of only one imaginary frequency.

The solvent effects of dioxane were taken into account in the thermodynamic calculations by full optimization of the in vacuo structures at the same computational level using the polarizable continuum model [37,38] in the framework of the self-consistent reaction field [39–41]. The values of M06-2X/6-311G(d,p) enthalpies, entropies, and Gibbs free energies in dioxane were calculated with standard statistical thermodynamics [36] at 293.15 °C and 1 atm by polarizable continuum model frequency calculations at the solvent-optimized structures. Except for the thermodynamic data, the rest of the results are obtained in in vacuo for an overall coherence in interpreting the results obtained using different quantum chemical tools.

DFT reactivity indices were calculated using the equations in [6]. The GEDT [13] values were computed using the equation $\text{GEDT}(f) = \sum q_f$, where q are the natural charges [42,43] of the atoms belonging to one of the two frameworks (f) at the TS geometries.

The Gaussian 16 suite of programs was used to perform the calculations [44]. Molecular geometries, ELF basin attractors, and the 3D representations of the Mulliken atomic spin densities were visualized by using the GaussView program [45]. ELF analyses [15] of the M06-2X/6-311G(d,p) monodeterminantal wavefunctions were performed by using the Top-Mod [46] package with a cubical grid of step size of 0.1 Bohr. The Bader's QTAIM [16,17] analyses were conducted using Multiwfn 3.7 software packages [47]. The IQA [35] analysis was performed with the AIMAll package [48] using the corresponding M06-2X/6-311G(d,p) monodeterminantal wavefunctions.

4. Conclusions

An IQA energy partitioning analysis of the TSs associated with the P-DA reactions of Cp **1** with the cyanoethylene series **2** permits to establish the decisive role of GEDT

in the acceleration found in polar reactions. The topological IQA energy partitioning allows establishing the complete linear correlation between the total IQA atomic energies of the electrophilic ethylene framework and the GEDT taking place at the TSs of these P-DA reactions. This finding establishes that the increase in GEDT at the TSs enhances the reaction rates of P-DA reactions through an electronic stabilization of the electrophilic framework.

The present MEDT study also shows that the asynchronicity in P-DA reactions depends on the non-symmetric electrophilic activation of the two interacting carbons of the ethylene caused by the electron-withdrawing substitution. A very good linear correlation between the geometric asynchronicity, Δl , at the TSs and the difference in the local electrophilicity ω_k indices of the C1 and C2 carbons of the cyanoethylenes, $\Delta\omega_k$, is found.

Supplementary Materials: The following supporting information can be downloaded at: <https://www.mdpi.com/article/10.3390/molecules29081870/s1>, ELF and QTAIM topological analysis of the TSs. References. Figure S1: with the M06-2X/6-311G(d,p) in vacuo ELF basin attractors together with the most relevant valence basin populations at Cp 1, ethylene 4 and the cyanoethylene series 2. Figure S2: with the M06-2X/6-311G(d,p) in vacuo the ELF basin attractors together with the most relevant valence basin populations at the TSs involved in the DA reactions of Cp 1 with ethylene 4 and the cyanoethylene series 2. Figure S3: with the representations of the contour-line maps of the Laplacian $\nabla^2\rho(r)$ of the electron density at the M06-2X/6-311G(d,p) in vacuo optimized TS-Et, TS-2CN and TS-4CN. Figure S4: with the plot of the computed M06-2X/6-311G(d,p) activation Gibbs free energies versus the number of cyano groups on the ethylene for the DA reactions of Cp 1 with the cyanoethylene series 2. Figure S5: with the plot of the logarithm of the experimental relative reaction rate constants versus the logarithm of the computed M06-2X/6-311G(d,p) relative reaction rate constants for the DA reactions of Cp 1 with the cyanoethylene series 2. Figure S6: with the M06-2X/6-311G(d,p) in vacuo optimized geometries of the TSs involved in the DA reactions of Cp 1 with ethylene 4 and the cyanoethylene series 2. Figure S7: with the plot of the in vacuo GEDT obtained by using Bader charges with respect to in vacuo GEDT obtained by using NPA charges. Figure S8: with the plot of the logarithm of the experimental reaction rate constants versus relative total IQA atomic energies stabilization of the ethylene framework for the DA reactions of Cp 1 with the cyanoethylene series 2. Table S1: with the M06-2X/6-311G(d,p) in vacuo QTAIM parameters of the (3,-1) CPs, as well as the dimensionless $|V(r)|/G(r)$ ratio, at the C1–C6 (CP1) and C2–C3 (CP2) interacting regions of the of the TSs involved in the DA reactions of Cp 1 with ethylene 4 and the cyanoethylene series 2. Table S2: with the M06-2X/6-311G(d,p) in vacuo total electronic energies of reagents, TSs and CAs involved in the DA reactions of Cp 1 with ethylene 4 and the cyanoethylene series 2. Table S3: with the M06-2X/6-311G(d,p) enthalpies, entropies and Gibbs free energies, computed at 293.15 K and 1 atm in dioxane, for the stationary points involved in the DA reactions of Cp 1 with ethylene 4 and the cyanoethylene series 2. Table S4: with distances between the C1–C6 and C2–C3 interacting carbons at the M06-2X/6-311G(d,p) optimized TSs in dioxane, geometrical asynchronicity, average of the two C–C interacting distances, and GEDT values. Table S5: with the total intra- and inter-atomic IQA energies at the diene and ethylene frameworks of the TSs and at the reagents involved in the DA reactions of Cp 1 with ethylene 4 and the cyanoethylene series 2. M06-2X/6-311G(d,p) g in vacuo computed total energies, single imaginary frequencies of TSs, and Cartesian coordinates of the stationary points involved in the DA reactions of Cp 1 with ethylene 4 and the cyanoethylene series 2 [49–60].

Author Contributions: Conceptualization, L.R.D.; methodology, L.R.D. and M.R.-G.; software, validation, L.R.D. and M.R.-G.; formal analysis, L.R.D. and M.R.-G.; investigation L.R.D. and M.R.-G.; data curation, L.R.D. and M.R.-G.; writing—original draft preparation, L.R.D. and M.R.-G.; writing—review and editing, L.R.D. and M.R.-G.; visualization, L.R.D. and M.R.-G. supervision, L.R.D. and M.R.-G. All authors have read and agreed to the published version of the manuscript.

Funding: This research received no external funding.

Data Availability Statement: The data that support the findings of this study are available from the corresponding author upon reasonable request.

Conflicts of Interest: The authors declare no conflicts of interest.

References

1. Ingold, C.K. Significance of tautomerism and of the reactions of aromatic compounds in the electronic theory of organic reactions. *J. Chem. Soc.* **1933**, 1120–1127. [[CrossRef](#)]
2. Lapworth, A. Replaceability of Halogen Atoms by Hydrogen Atoms. *Nature* **1925**, *115*, 625.
3. Carey, F.A.; Sundberg, R.J. *Advanced Organic Chemistry, Part A: Structure and Mechanisms*; Springer: New York, NY, USA, 2008.
4. Parr, R.G.; Szentpaly, L.V.; Liu, S. Electrophilicity index. *J. Am. Chem. Soc.* **1999**, *121*, 1922–1924. [[CrossRef](#)]
5. Parr, R.G.; Yang, W. *Density Functional Theory of Atoms and Molecules*; Oxford University Press: New York, NY, USA, 1989.
6. Domingo, L.R.; Ríos-Gutiérrez, M.; Pérez, P. Applications of the conceptual density functional indices to organic chemistry reactivity. *Molecules* **2016**, *21*, 748. [[CrossRef](#)] [[PubMed](#)]
7. Domingo, L.R.; Aurell, M.J.; Pérez, P.; Contreras, R. Quantitative characterization of the global electrophilicity power of common diene/dienophile pairs in Diels–Alder reactions. *Tetrahedron* **2002**, *58*, 4417–4423. [[CrossRef](#)]
8. Domingo, L.R.; Chamorro, E.; Pérez, P. Understanding the reactivity of captodative ethylenes in polar cycloaddition reactions. A theoretical study. *J. Org. Chem.* **2008**, *73*, 4615–4624. [[CrossRef](#)]
9. Domingo, L.R.; Ríos-Gutiérrez, M. In Application of Reactivity Indices in the Study of Polar Diels–Alder Reactions. In *Conceptual Density Functional Theory: Towards a New Chemical Reactivity Theory*; Liu, S., Ed.; WILEY-VCH GmbH: Weinheim, Germany, 2022; Volume 2, pp. 481–502.
10. Sauer, J.; Wiest, H.; Mielert, A. Eine Studie der Diels-Alder-Reaktion, I. Die Reaktivität von Dienophilen gegenüber Cyclopentadien und 9.10-Dimethyl-anthracen. *Chem. Ber.* **1964**, *97*, 3183–3207. [[CrossRef](#)]
11. Domingo, L.R.; Aurell, M.J.; Pérez, P.; Contreras, R. Origin of the synchronicity on the transition structures of polar Diels–Alder reactions. Are these reactions [4+2] processes? *J. Org. Chem.* **2003**, *68*, 3884–3890. [[CrossRef](#)] [[PubMed](#)]
12. Jones, G.O.; Guner, V.A.; Houk, K.N. Diels–Alder Reactions of Cyclopentadiene and 9,10-Dimethylanthracene with Cyanoalkenes: The Performance of Density Functional Theory and Hartree-Fock Calculations for the Prediction of Substituent Effects. *J. Phys. Chem. A* **2006**, *110*, 1216–1224. [[CrossRef](#)]
13. Domingo, L.R. A new C–C bond formation model based on the quantum chemical topology of electron density. *RSC Adv.* **2014**, *4*, 32415–32428. [[CrossRef](#)]
14. Domingo, L.R.; Sáez, J.A. Understanding the mechanism of polar Diels–Alder reactions. *Org. Biomol. Chem.* **2009**, *7*, 3576–3583. [[CrossRef](#)] [[PubMed](#)]
15. Becke, A.D.; Edgecombe, K.E. A simple measure of electron localization in atomic and molecular systems. *J. Chem. Phys.* **1990**, *92*, 5397–5403. [[CrossRef](#)]
16. Bader, R.F.W.; Tang, Y.H.; Tal, Y.; Biegler-König, F.W. Properties of atoms and bonds in hydrocarbon molecules. *J. Am. Chem. Soc.* **1982**, *104*, 946–952. [[CrossRef](#)]
17. Bader, R.F.W. *Atoms in Molecules: A Quantum Theory*; Oxford University Press: Oxford, NY, USA, 1994.
18. Domingo, L.R.; Ríos-Gutiérrez, M.; Pérez, P. How does the global electron density transfer diminish activation energies in polar cycloaddition reactions? A Molecular Electron Density Theory study. *Tetrahedron* **2017**, *73*, 1718–1724. [[CrossRef](#)]
19. Domingo, L.R. Molecular Electron Density Theory: A Modern View of Reactivity in Organic Chemistry. *Molecules* **2016**, *21*, 1319. [[CrossRef](#)] [[PubMed](#)]
20. Fukui, K. *Molecular Orbitals in Chemistry, Physics, and Biology*; Academic Press: New York, NY, USA, 1964.
21. Kitaura, K.; Morokuma, K. A new energy decomposition scheme for molecular interactions within the Hartree-Fock approximation. *Int. J. Quantum Chem.* **1976**, *10*, 325–340. [[CrossRef](#)]
22. Morokuma, K.; Kitaura, K. *Chemical Applications of Atomic and Molecular Electrostatic Potentials*; Plenum: New York, NY, USA, 1981; pp. 215–242.
23. Blanco, M.A.; Martín Pendás, A.; Francisco, E. Interacting Quantum Atoms: A Correlated Energy Decomposition Scheme Based on the Quantum Theory of Atoms in Molecules. *J. Chem. Theory Comput.* **2005**, *1*, 1096–1109. [[CrossRef](#)] [[PubMed](#)]
24. Domingo, L.R.; Ríos-Gutiérrez, M.; Pérez, P. Why is Phenyl Azide so Unreactive in [3+2] Cycloaddition Reactions? Demystifying Sustmann’s Paradigmatic Parabola. *Org. Chem. Front.* **2023**, *10*, 5579–5591. [[CrossRef](#)]
25. Domingo, L.R.; Pérez, P.; Ríos-Gutiérrez, M.; Aurell, M.J. A Molecular Electron Density Theory Study of Hydrogen Bond Catalysed Polar Diels–Alder Reactions of α , β -unsaturated Carbonyl Compounds. *Tetrahedron Chem.* **2024**, *10*, 100064. [[CrossRef](#)]
26. Parr, R.G.; Pearson, R.G. Absolute hardness: Companion parameter to absolute electronegativity. *J. Am. Chem. Soc.* **1983**, *105*, 7512–7516. [[CrossRef](#)]
27. Domingo, L.R.; Ríos-Gutiérrez, M.; Pérez, P. A Molecular Electron Density Theory Study of the Reactivity of Tetrazines in Aza-Diels–Alder Reactions. *RSC Adv.* **2020**, *10*, 15394–15405. [[CrossRef](#)]
28. Domingo, L.R.; Ríos-Gutiérrez, M. A Useful Classification of Organic Reactions Bases on the Flux of the Electron Density. *Sci. Rad.* **2023**, *2*, 1. [[CrossRef](#)]
29. Domingo, L.R.; Pérez, P.; Sáez, J.A. Understanding the local reactivity in polar organic reactions through electrophilic and nucleophilic Parr functions. *RSC Adv.* **2013**, *3*, 1486–1494. [[CrossRef](#)]
30. Domingo, L.R.; Aurell, M.J.; Pérez, P.; Contreras, R. Quantitative characterization of the local electrophilicity of organic molecules. Understanding the regioselectivity on Diels–Alder reactions. *J. Phys. Chem. A* **2002**, *106*, 6871–6875. [[CrossRef](#)]
31. Evans, M.G.; Polanyi, M. Some applications of the transition state method to the calculation of reaction velocities, especially in solution. *Trans. Faraday Soc.* **1935**, *31*, 875–894. [[CrossRef](#)]

32. Woodward, R.B. The mechanism of the Diels-Alder reaction. *J. Am. Chem. Soc.* **1942**, *64*, 3058–3059. [CrossRef]
33. Triestram, L.; Falcioni, F.; Popelier, P.L.A. Interacting Quantum Atoms and Multipolar Electrostatic Study of $XH\cdots\pi$ Interactions. *ACS Omega* **2023**, *8*, 34844–34851. [CrossRef]
34. Chattaraj, P.K.; Roy, D.R. Update 1 of: Electrophilicity Index. *Chem. Rev.* **2007**, *107*, PR46–PR74. [CrossRef]
35. Zhao, Y.; Truhlar, D.G. The M06 suite of density functionals for main group thermochemistry, thermochemical kinetics, noncovalent interactions, excited states, and transition elements: Two new functionals and systematic testing of four M06-class functionals and 12 other functionals. *Theor. Chem. Acc.* **2008**, *120*, 215–245.
36. Hehre, M.J.; Radom, L.; Schleyer, P.V.R.; Pople, J. *Ab Initio Molecular Orbital Theory*; Wiley: New York, NY, USA, 1986.
37. Tomasi, J.; Persico, M. Molecular interactions in solution: An overview of methods based on continuous distributions of the solvent. *Chem. Rev.* **1994**, *94*, 2027–2094. [CrossRef]
38. Simkin, B.Y.; Sheikhet, I.I. *Quantum Chemical and Statistical Theory of Solutions—Computational Approach*; Ellis Horwood: London, UK, 1995.
39. Cossi, M.; Barone, V.; Cammi, R.; Tomasi, J. Ab initio study of solvated molecules: A new implementation of the polarizable continuum model. *Chem. Phys. Lett.* **1996**, *255*, 327–335. [CrossRef]
40. Cancès, E.; Mennucci, B.; Tomasi, J. A new integral equation formalism for the polarizable continuum model: Theoretical background and applications to isotropic and anisotropic dielectrics. *J. Chem. Phys.* **1997**, *107*, 3032–3041. [CrossRef]
41. Barone, V.; Cossi, M.; Tomasi, J. Geometry optimization of molecular structures in solution by the polarizable continuum model. *J. Comput. Chem.* **1998**, *19*, 404–417. [CrossRef]
42. Reed, A.E.; Weinstock, R.B.; Weinhold, F. Natural population analysis. *J. Chem. Phys.* **1985**, *83*, 735–746. [CrossRef]
43. Reed, A.E.; Curtiss, L.A.; Weinhold, F. Intermolecular interactions from a natural bond orbital, donor-acceptor viewpoint. *Chem. Rev.* **1988**, *88*, 899–926. [CrossRef]
44. Frisch, M.J.; Trucks, G.W.; Schlegel, H.B.; Scuseria, G.E.; Robb, M.A.; Cheeseman, J.R.; Scalmani, G.; Barone, V.; Petersson, G.A.; Nakatsuji, H.; et al. *Gaussian 16, Revision A.03*; Gaussian, Inc.: Wallingford, CT, USA, 2016.
45. Dennington, R.; Keith, T.A.; Millam, J.M. *GaussView*, 6th ed.; Semichem Inc.: Shawnee Mission, KS, USA, 2016.
46. Noury, S.; Krokidis, X.; Fuster, F.; Silvi, B. Computational tools for the electron localization function topological analysis. *Comput. Chem.* **1999**, *23*, 597–604. [CrossRef]
47. Lu, T.; Chen, F. Multiwfn: A multifunctional wavefunction analyzer. *J. Comp. Chem.* **2012**, *33*, 580–592. [CrossRef]
48. Keith, T.A. *TK Gristmill Software, AIMAll (Version 19.10.12)*; Gristmill Software: Overland Park, KS, USA, 2019. Available online: www.aim.tkgristmill.com (accessed on 15 April 2024).
49. Wilson, A.L.; Popelier, P.L.A. Exponential Relationships Capturing Atomistic Short-Range Repulsion from the Interacting Quantum Atoms (IQA) Method. *J. Phys. Chem. A* **2016**, *120*, 9647–9659. [CrossRef] [PubMed]
50. Popelier, P.L.A.; Kosov, D.S. Atom–atom partitioning of intramolecular and intermolecular Coulomb energy. *J. Chem. Phys.* **2001**, *114*, 6539–6547. [CrossRef]
51. Popelier, P.L.A.; Joubert, L.; Kosov, D.S. Convergence of the Electrostatic Interaction Based on Topological Atoms. *J. Phys. Chem. A* **2001**, *105*, 8254–8261. [CrossRef]
52. Martín Pendás, A.; Francisco, E.; Blanco, M.A.; Gatti, C. Bond Paths as Privileged Exchange Channels. *Chem. Eur. J.* **2007**, *13*, 9362–9371. [CrossRef] [PubMed]
53. Berski, S.; Andrés, J.; Silvi, B.; Domingo, L.R. The joint use of catastrophe theory and electron localization function to characterize molecular mechanisms. A density functional study of the Diels-Alder reaction between ethylene and 1,3-butadiene. *J. Phys. Chem. A* **2003**, *107*, 6014–6024. [CrossRef]
54. Domingo, L.R.; Ríos-Gutiérrez, M.; Silvi, B.; Pérez, P. The Mysticism of Pericyclic Reactions: A Contemporary Rationalisation of Organic Reactivity Based on Electron Density Analysis. *Eur. J. Org. Chem.* **2018**, *2018*, 1107–1120. [CrossRef]
55. Domingo, L.R.; Pérez, P.; Sáez, J.A. Origin of the synchronicity in bond formation in polar Diels-Alder reactions: An ELF analysis of the reaction between cyclopentadiene and tetracyanoethylene. *Org. Biomol. Chem.* **2012**, *10*, 3841–3851. [CrossRef] [PubMed]
56. Domingo, L.R.; Sáez, J.A.; Zaragoza, R.J.; Arnó, M. Understanding the Participation of Quadricyclane as Nucleophile in Polar $[2\sigma + 2\sigma + 2\pi]$ Cycloadditions toward Electrophilic π Molecules. *J. Org. Chem.* **2008**, *73*, 8791–8799. [CrossRef] [PubMed]
57. Woodward, R.B.; Hoffmann, R. The Conservation of Orbital Symmetry. *Angew. Chem. Int. Ed. Engl.* **1969**, *8*, 781–853. [CrossRef]
58. Houk, K.N.; González, J.; Li, Y. Pericyclic reaction transition states: Passions and punctilios, 1935–1995. *Acc. Chem. Res.* **1995**, *28*, 81–90. [CrossRef]
59. Domingo, L.R.; Ríos-Gutiérrez, M.; Chamorro, E.; Pérez, P. Aromaticity in Pericyclic Transition State Structures? A Critical Rationalisation Based on the Topological Analysis of Electron Density. *ChemistrySelect* **2016**, *1*, 6026–6039. [CrossRef]
60. Espinosa, E.; Alkorta, I.; Elguero, J.; Molins, E. From weak to strong interactions: A comprehensive analysis of the topological and energetic properties of the electron density distribution involving $X-H\cdots F-Y$ systems. *J. Chem. Phys.* **2002**, *117*, 5529–5542. [CrossRef]

Disclaimer/Publisher’s Note: The statements, opinions and data contained in all publications are solely those of the individual author(s) and contributor(s) and not of MDPI and/or the editor(s). MDPI and/or the editor(s) disclaim responsibility for any injury to people or property resulting from any ideas, methods, instructions or products referred to in the content.